Applied Research Laboratory

Technical Report

EXPANSION OF KEMP-SEARS UNSTEADY LIFT
PREDICTOR FOR TURBOMACHINERY

by

P. D. Lysak
R. C. Marboe

PENNSTATE

1855
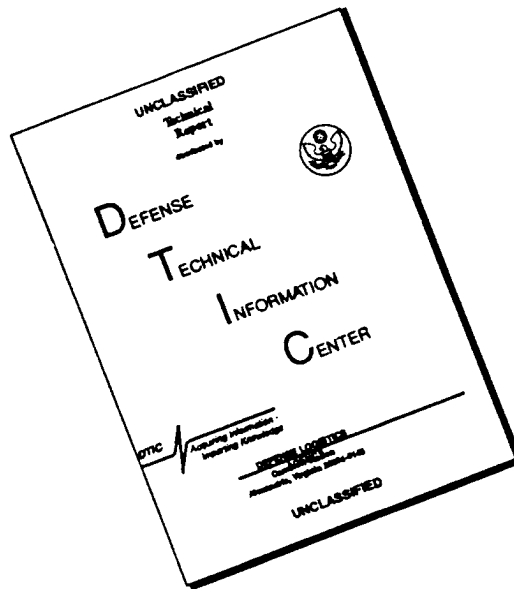
DISCLAIMER NOTICE

THIS DOCUMENT IS BEST QUALITY AVAILABLE. THE COPY FURNISHED TO DTIC CONTAINED A SIGNIFICANT NUMBER OF PAGES WHICH DO NOT REPRODUCE LEGIBLY.

The Pennsylvania State University
APPLIED RESEARCH LABORATORY
P.O. Box 30
State College, PA 16804

EXPANSION OF KEMP-SEARS UNSTEADY LIFT
PREDICTOR FOR TURBOMACHINERY

by

P. D. Lysak
R. C. Marboe

Technical Report No. TR 96-004
May 1996

19960530 083

REPORT DOCUMENTATION PAGE

1. AGENCY USE ONLY (Leave blank)	2. REPORT DATE	3. REPORT TYPE AND DATES COVERED
	May 1996	B.S. Honors Thesis in Engineering Science

4. TITLE AND SUBTITLE

Expansion of Kemp-Sears Unsteady Lift Predictor for Turbomachinery

5. FUNDING NUMBERS

6. AUTHOR(S)

P. D. Lysak and R. C. Marboe

7. PERFORMING ORGANIZATION NAME(S) AND ADDRESS(ES)

Applied Research Laboratory
The Pennsylvania State University
PO Box 30
State College, PA 16804

8. PERFORMING ORGANIZATION REPORT NUMBER

TR# 96-004

9. SPONSORING / MONITORING AGENCY NAME(S) AND ADDRESS(ES)

Mr. Robert Fry
Code SEA 92RE1
Naval Sea Systems Command
2531 Jefferson Davis Highway
Arlington, VA 22242-5160

10. SPONSORING / MONITORING AGENCY REPORT NUMBER

11. SUPPLEMENTARY NOTES

12a. DISTRIBUTION / AVAILABILITY STATEMENT

Approved for Public Release; Distribution Unlimited

12b. DISTRIBUTION CODE

13. ABSTRACT (Maximum 200 words)

A computer model which evaluates the unsteady forces acting on a three-dimensional blade has been developed using the theory of Kemp and Sears (1953, 1955). Based on an existing computer model which performed unsteady lift calculations for a two-dimensional cascade of airfoils, the expanded model breaks the three-dimensional stator and rotor blades into a series of radial sections which are then evaluated as two-dimensional cascades. A user of the model can investigate how the magnitude and phase of the unsteady lift changes along the radius of the blade and determine the total unsteady blade forces acting in the axial and tangential directions. The computer model has been implemented in Mathcad ® version 6.0+, by MathSoft Inc., and can be used as an interactive design tool.

The theory and implementation of the prediction model are discussed in this document. A brief overview of the Kemp-Sears theory and its simplifying assumptions is presented before a more thorough discussion of the three-dimensional blade geometry and the steps involved in breaking it down into cascade sections. In addition, the benefits of using Mathcad to implement the model are mentioned, and some ways of using the predictor are recommended.

14. SUBJECT TERMS

propeller unsteady forces; turbomachinery design; unsteady lift

15. NUMBER OF PAGES

50

16. PRICE CODE

17. SECURITY CLASSIFICATION OF REPORT	18. SECURITY CLASSIFICATION OF THIS PAGE	19. SECURITY CLASSIFICATION OF ABSTRACT	20. LIMITATION OF ABSTRACT
Unclassified	Unclassified	Unclassified	

ABSTRACT

A computer model which evaluates the unsteady forces acting on a three-dimensional blade has been developed using the theory of Kemp and Sears (1953, 1955). Based on an existing computer model which performed unsteady lift calculations for a two-dimensional cascade of airfoils, the expanded model breaks the three-dimensional stator and rotor blades into a series of radial sections which are then evaluated as two-dimensional cascades. A user of the model can investigate how the magnitude and phase of the unsteady lift changes along the radius of the blade and determine the total unsteady blade forces acting in the axial and tangential directions. The computer model has been implemented in Mathcad ® version 6.0+, by MathSoft Inc., and can be used as an interactive design tool.

The theory and implementation of the prediction model are discussed in this document. A brief overview of the Kemp-Sears theory and its simplifying assumptions is presented before a more thorough discussion of the three-dimensional blade geometry and the steps involved in breaking it down into cascade sections. In addition, the benefits of using Mathcad to implement the model are mentioned, and some ways of using the predictor are recommended.

TABLE OF CONTENTS

Page Number

LIST OF TABLES

LIST OF FIGURES

INTRODUCTION

Unsteady flow phenomenon is an important consideration in the design of quiet turbomachinery. Relative motion between blade rows causes periodic fluctuation in the flow through a turbomachine stage, which leads to unsteady forces acting on the blades. Determining the nature of the unsteady forces is complicated, and many approaches to solving the problem have been suggested. Kemp & Sears (1953,1955) developed a theory which predicts the generated unsteady forces through calculation of the interference between a stator and rotor using unsteady airfoil theory. These calculations are very involved and require a computer to efficiently solve for the unsteady forces. In addition, determining the total unsteady forces for an actual stator and rotor involves breaking down the blades into spanwise sections which can be evaluated by the theory and then summed.

An ARL computer program, based on original work by Sevik (1966), has been in existence for many years to perform the Kemp & Sears calculations. However, this program was limited to the case of two-dimensional airfoils and did not make realistic predictions for actual stators and rotors. To solve this problem, an expanded computer model was developed which takes into consideration the three-dimensional nature of the problem. Instead of solving for cascaded 2D airfoils, the new model evaluates the lift covering a three-dimensional blade span, so it is able to predict the total unsteady forces in both the axial and tangential directions on the blades of the stator and rotor.

The other motivation for developing a new model was to create the model in a mathematical computing environment, so the calculations could be easily seen and understood. The model was written using Mathcad ® version 6.0+, by MathSoft Inc., which provides an interactive user interface, graphical output features, and flexibility for processing input and output. Using Mathcad has made the predictor more powerful through the addition of graphical features and clear organization.

BACKGROUND

Unsteady Lift Theory

The model computes the unsteady lift and moment acting on radial sections of the blades of a stator-rotor stage and the total unsteady forces (axial and tangential components) acting on the entire blade span. The unsteady lift model is based on the theory of Kemp & Sears. First, Sears (1941) developed a theory to predict the unsteady lift acting on a single thin airfoil due to a sinusoidally varying inflow. Then this unsteady airfoil theory was used by Kemp & Sears (1953, 1955) in developing a theory to predict the unsteady lift acting on the blades of a stator and rotor stage. The theory accounts for the periodic interaction between the stator and rotor rows due to their motion relative to each other. This interaction results in an unsteady flow field around the blades, from which an unsteady lift is found using the Sears unsteady airfoil theory.

The Kemp & Sears theory used many assumptions to simplify a complicated problem. First, the stator and rotor rows were represented as an infinitely long cascade of two-dimensional, thin airfoils. This eliminated the radially dependent features of the flow and the blade geometry. In the present model, which uses three-dimensional stator and rotor rows, the cascade representation is used to represent radial sections of the three-dimensional geometry.

The other simplifications used in the Kemp & Sears theory deal with the airfoils and flow properties. First, thin airfoil theory is used, which is restricted to airfoils with small thickness, camber, and angle of attack. Second, the fluid in the theory is idealized as an inviscid, incompressible fluid, as is customarily done for thin airfoil theory. A more restrictive assumption, a consequence of using the cascade representation of two-dimensional airfoils, is that the flow leaving the stator airfoils is parallel to the moving rotor airfoils (Figure 1). However, a constant angle of attack on the rotor airfoils can be set if it is known. Because of this flow assumption, the velocities of flow relative to the stator and rotor are functions of the rotor RPM and the stator and rotor stagger angles.

Keeping these assumptions in mind, the Kemp & Sears theory calculates the unsteady lift acting on the stator and rotor rows of two-dimensional airfoils. The upstream stator row has an unsteady lift caused solely by the periodic fluctuation in circulation around the airfoil due to the motion of the rotor. The unsteady lift on the rotor row is calculated from three effects. First, the rotor encounters an effect similar to the stator caused by the fluctuation in circulation around the airfoil due to the relative motion of the stator past the rotor. The other two effects account for the wakes of the stator row. The second rotor effect accounts for the fluctuation in the rotor's circulation due to the rotor passing periodically through the vortices of the stator's wake. The third rotor effect, developed in Kemp & Sears' second paper (1955) accounts for the periodic passage of the rotor through the viscous wakes shed by the stator. The viscous wake is modeled using an empirical equation based on the drag coefficient of the stator, and is superimposed on the inviscid flow used for the rest of the theory. Once these three unsteady lift effects are calculated, the unsteady lift on the rotor blades is found by the summation of the three complex quantities.

Extension of 2D Airfoils to 3D Blades

In order to make a more realistic unsteady lift model of a stator-rotor stage, the Kemp & Sears theory has been applied to a three-dimensional stator-rotor stage. The two-dimensional cascade theory is used to represent radial sections of a three-dimensional stator-rotor geometry. The stator-rotor rows are broken up into a set of radial sections starting at the hub and extending outward to the blade tip. Each section is represented as a two-dimensional cascade as in the Kemp & Sears theory, but the geometry of the cascade (stagger angles, chord length, separation of blades, distance between rows) changes to reflect the three-dimensional geometry of the blade rows being modeled. As will be seen later, this has a large impact on the total unsteady lift predicted for a blade.

The stator and rotor blades are defined by a set of radial sections, each of which contains a radius, chord length, stagger angle, skew, and rake. The cascade representation is defined by the parameters of chord length, spacing between adjacent blades, stagger angle, and axial spacing between blade rows. Two of these parameters are already defined by the blade geometry. The blade-to-blade spacing is computed by dividing the section circumference by the number of blades. The axial spacing is affected by the rake of each section. The skew of the blades is not used as a cascade parameter, but is used to adjust the phase of the section's unsteady lift relative to other radial sections.

Using the Kemp-Sears theory, the unsteady lift coefficient of each radial section is computed from the cascade representation of the section. This unsteady lift coefficient is a complex vector directed normal to the chord direction and acting at the mid-chord point. The next step is to find the total unsteady forces acting on the entire blade span from hub to tip. First, each section's unsteady lift coefficient is converted to an actual lift per span. The lift per span is then multiplied by the span of the radial strip, and vector summation is used to total the unsteady forces. The unsteady forces are calculated for both the axial (thrust) and tangential (side force) directions.

Since totaling the lift involves a summation of complex numbers, the phase at each section has a big impact on the total unsteady forces acting on each blade. Designing the blade so that the lift at one end of the blade is out of phase with the other end is a good way to lower the average unsteady lift of the blade. The ability to account for the phase differences across the span of the blade helps make the current model more realistic than the original Kemp & Sears theory. Nearly every blade will have some phase contribution in the average unsteady lift because the blade-to-blade spacing gets bigger as the radius gets bigger. Also, designing radial variations in the stagger angles and chord lengths, and adding rake and skew to the blade, will cause the phase of the unsteady lift to vary with radius.

IMPLEMENTATION OF THE PREDICTOR

The three-dimensional Kemp & Sears unsteady lift prediction model has been implemented as a Mathcad version 6.0+ document. Using this document, an engineer can test a prospective stator-rotor stage and get quick turn around of the predicted unsteady lift and moment on the stator and rotor blades and the unsteady rotor thrust. In addition, the user of the document can design interactively using changes in the geometry to see how different modifications change the level of unsteadiness. A discussion of the objectives, layout, use, and reliability of the Mathcad implementation of the unsteady prediction model follows. Also, the nomenclature for the predictor is listed in Appendix 1, and a listing of the Mathcad document can be found in Appendix 2.

Reasons for Using Mathcad

There were several reasons for implementing the prediction model in Mathcad. First, Mathcad allows the user to work with mathematical equations, instead of a programming code. This feature is extremely beneficial when the equations become very complicated, as they do in the Kemp & Sears theory. In the Mathcad implementation of the predictor, most of the variables keep the same symbols that were used in the Kemp & Sears paper. This helps ensure that the equations are correct. As a matter of fact, several errors in older FORTRAN implementations of the Kemp & Sears theory were found when creating the Mathcad document. Unmanageable equations that were spread out over several lines of FORTRAN code, with multiple levels of parentheses and function calls, became clear and orderly when implemented in Mathcad.

The second advantage Mathcad provided was the ability to make a clear document layout. Using section headings and page breaks, the document was organized to make it easy to both use and study. For ease of use, the input and output sections are contained on the first several pages. The calculation sections come behind the input and output so they do not have to be seen or printed every time the document is used. The calculations are broken up into geometry variable definition, function definition, Kemp & Sears theory implementation, interpolation and splining, complex summation, thrust, and verification sections. Of particular interest is the Kemp & Sears theory implementation section, which is subdivided into separate pages for each contribution to the unsteady lift. Each equation used from the theory contains a reference to the equation number in the Kemp & Sears papers where the equation is first presented. These references are included both for verification of the equations and to help users who would like to study how the predictor works.

The third advantage in using Mathcad is the flexible input and output. A file format has been developed to store the stator and rotor geometry information and to read it into Mathcad, but sometimes the information might be stored in a different format. Using the Windows clipboard cut-and-paste, data can be imported into any Mathcad variable quickly and easily. Also, the geometry data can be changed be redefining a variable inside the Mathcad document, which is an easy way to test the effect of modifications to the design. An example would be using a multiplying factor times the skew variable to increase or decrease the total skew over the rotor blade span.

Just like the input, the output is also flexible. The standard output developed for the document is a set of plots of the unsteady lift vs. radius and tables of the unsteady thrust and side forces for the first few harmonics. However, additional insight into the problem can be gained by looking at other quantities, such as the rotor unsteady lift produced by the three effects individually. This shows whether the interference or viscous effect is causing the most unsteady lift, which could help a designer figure out how to modify the geometry. In addition, if the unsteady lift results do not make sense, the intermediate values in the calculation section can be displayed one at a time, allowing the user to trace through the calculations and diagnose any problems.

Finally, having the document clearly organized and the equations understandable makes it easier to modify the model in the future. Some possible changes include redefining the viscous wake in order to better match the problem being studied and modifying the Sears unsteady lift formula to account for the thickness profile and camber of the blade.

Input Set

The input section of the predictor can be grouped into two categories: control parameters and stator/rotor blade descriptions. First, the control parameters include the number of harmonics to be computed, the axial spacing between the stator and rotor, the rotor RPM, the free-stream reference velocity, and the fluid density (Table 1). The unsteady lift is calculated for a series of harmonics, which correspond to multiples of the frequency of the rotor's revolution times the number of rotor blades (for the unsteady lift on the stator blades) or times the number of stator blades (for the unsteady lift on the rotor blades). The unsteady lift generally decreases in magnitude quickly for higher harmonics, so the first few are probably the ones of greatest interest. If more than about five or six harmonics are computed, the document may take a while to calculate.

Second, the blade descriptions contain most of the data used for the predictions. A few quantities need to be entered by hand, but most of the data is read from the blade profile files. The hand-entered quantities are the number of blades for each row, the tip radius and hub radius of each row, and the stator drag coefficient (Table 2). The tip and hub radii are measured from the axial centerline, and the tip radius is used to normalize the data in the blade file.

The blade file (Table 3) contains nine fields per radial section of the blade. The file must be in ASCII format and contain one line per radial section, since the number of the radial sections is determined from the number of data lines in the file. A text header of one or more lines is optional, but all text must come before any number fields. The nine fields on each line can be delimited by spaces, tabs, or commas. Since this file format is used for other applications in addition to the Kemp & Sears Predictor, some of the fields in the file are not used by the predictor. These fields can be filled with any number, but must be entered for the file to be read properly. Figure 4 shows some examples of valid and invalid files formats.

The other parameters which can be changed if desired are the steady bound-vortex distribution coefficients, which correspond to the shape and angle of attack of the cross-sectional airfoil. These coefficients are defaulted to use an elliptic load distribution, which works for airfoils that have a symmetric camber profile and no angle of attack. The coefficients can be changed if greater accuracy is desired and the exact camber profile is known. The coefficients are computed using the formulas:

$$A0 = \alpha - \frac{1}{\pi}\int_0^\pi \frac{dY(\theta)}{dX}d\theta \qquad\qquad A1 = \frac{2}{\pi}\int_0^\pi \frac{dY(\theta)}{dX}\cos(\theta)d\theta$$

where: y = camber
         x = coordinate along chord line
         θ = angle to X,Y with origin at mid-chord
         α = angle of attack

The variables are defined at the beginning of the calculation section of the document, right before the rotor geometry interpolation.

Interpolation

After the input is read, the next step is to convert the data so that the stator and rotor sections have the same radii. This could be done when creating the blade input files, but often it is not convenient to do so, and the document does not require it. The radial sections of the stator are chosen as the radii which will be used to form the cascade models, and the rotor section data is interpolated, using cubic splines, to sections

corresponding to the stator radii (Figure 3). This sets up the model so it is ready to form cascade representations of the radial sections. It is important to note that the model is making the simplification that the interaction between the blade rows occurs at one radius.

Conversion to Cascade

The Kemp & Sears theory is based on a cascade representation of the blade rows. The model takes the geometry, and after interpolating the rotor so the radial sections correspond to the stator sections, converts the geometric blade properties to cascade parameters (Table 4). The cascade representation is made up of stagger angles, semi-chord lengths, the distances between adjacent blades in the same row, skews, and the distance between the blade rows. A cascade representation is formed for each radial section to reflect the geometry of the blades at that section. The single cascade theory of Kemp & Sears theory is used multiple times, once for each cascade in the model. Using this theory, the stator and rotor unsteady lift, which is a complex quantity with magnitude and phase, is calculated for each radial section. The model uses the variation of the unsteady lift along the blade to compute an average lift for the blade.

One cascade parameter worth discussing further is the skew. Since the Kemp & Sears theory was for only one section, the skew was not included. However, in a three-dimensional model it is important to include it. Briefly, skew is a measure of the amount of tangential offset in the blade as you move outward along the blade radius. As a sign convention, positive skew corresponds to an offset in the direction opposite to the direction of rotation (the rotor rotation direction is used for both the stator and the rotor blades). The effect of the skew is to shift the phase of the unsteady lift calculated at the section. For example, a positive rotor skew results in a negative phase shift by the amount of the skew angle on the unsteady lift of the rotor. Since skew can be present on both the rotor and stator blades, the difference, or net skew, is calculated. For the shift on the stator blade, the rotor skew is subtracted from the stator skew; for the shift on the rotor blade, it is the opposite. The net skew is then accounted for by adding it onto the phase of the unsteady lift. This step is performed each time the unsteady lift is computed, so it is done once for the stator and three times for the rotor.

Calculation Section

Once the input data and blade geometry are converted into cascade sections, the model uses the Kemp & Sears theory to calculate the unsteady lift and moment at each section. The calculation section is organized into several sections, beginning with the definition of the aerodynamic functions used, sections for each unsteady lift effect calculated (one for the stator and three for the rotor), and ending with the summation of the lift for the blade. When a calculation is based on the Kemp & Sears theory, a reference to the page and equation number is included. The implementation of the calculations can be seen by looking at the Mathcad document included in the appendix.

Output and Results

The main output features of the document are the plots of the magnitude and phase of the stator and rotor unsteady lift vs. normalized radius (shown for one harmonic at a time), and the tables and plots of the total axial and tangential unsteady force acting on an entire blade (shown in lift coefficient form) for every harmonic. This output shows both the change in the unsteady lift with position on the blade and the change in the total unsteady lift with harmonic. In addition, the unsteady lift vs. radius plots can be helpful in understanding where the total unsteady lift values come from. For example, the sections of the blade which have the highest unsteady lift could be addressed in a re-design to lower the total unsteady lift of the blade. Also, if the phase is nearly constant for the span the average unsteady lift will be higher than if part of the lift is out of phase with the lift at other radii. Since skew causes a phase shift in the unsteady lift, the skew could be altered to produce a desired unsteady lift.

One of the advantages of using Mathcad is the ability to quickly modify the document to see additional output in the form of tables and plots. This can be used to supplement the basic output of the document. For example, it may be useful to look at plots of the aerodynamic functions, the intermediate functions used to calculate the lift, or the individual components of the rotor lift. Other possibilities include overlay plots, such as the unsteady lift overlaid with the skew or another geometric property.

ANALYSIS OF THE PREDICTIONS

In order to use the predictor effectively, it will be helpful to know a little bit about what controls the results of the predictions and how to ensure that the predictions are accurate. This section explains what geometric properties should be given the most attention when looking for ways to reduce the unsteady lift and points out some things to be careful of when creating the geometry input files.

The biggest influence on the magnitude of the unsteady lift is generally the axial spacing between the blade rows. As the rows are spaced further apart, the amount of potential interaction between the blades decreases, so the unsteady lift also decreases. The interaction between the blade rows also depends on the number of blades in each row. For a constant stator blade lift, the fewer the number of stator blades, the less important the interference effects become, so the viscous wake effect dominates the unsteady lift. In these cases, the separation of the blade rows may have less control over the magnitude of the unsteady lift than the geometric properties and drag of the stator blades.

The second most important thing to consider is the distribution of the geometry points which define the blade shape. Since computing the total blade unsteady lift involves a summation of all the unsteady lifts (both magnitude and phase) at the radial sections calculated, the total depends a lot on how variable the phase is. The total unsteady lift is often quite a bit less than the magnitude of the unsteady lift at any one radial section, since the unsteady lift at some radial sections will be out of phase with other sections and end up canceling each other out. It is important to cover as much of the blade span as possible to accurately determine the amount of phase cancellation and get an accurate total unsteady lift. Also, the greater the number of sections calculated, the thinner each strip and more accurate the totals.

Another thing to consider is which stator section is interacting with which rotor section. Since the model calculates the interaction of one stator section with one rotor section, it is important to have the correct ones matching. The model assumes that there is negligible radial flow, so the stator interacts with the rotor at points at the same radii. Some applications may involve the stator and rotor being mounted on a sloping

surface, and a correction can be made to account for a body cone angle. To make this correction, the rotor radii should be shifted inward from the stator radii by subtracting the slope of the cone angle times the axial spacing between the rows. Note that this assumes that the radial component of the flow follows the cone angle.

The last consideration when using the model is the viscous wake effect. In some situations, such as when there are relatively few stator blades, this effect can dominate, so it is important that the wake is determined accurately. The calculation of the wake is primarily controlled by the drag coefficient of the stator, which is used in an empirical equation. To improve the accuracy of this calculation, a more recent empirical expression could be substituted.

RECOMMENDATIONS

When using the predictor, it is important to keep in mind the assumptions and simplifications that have been made. Because of these simplifications, the unsteady lift values should not be relied upon as accurate values of the actual unsteady lift until proper validation against experimental results has been accomplished. However, the predictor can be used as a valuable tool to investigate how changes in the stator-rotor geometry affect the unsteady lift and forces. The predictor is at present most useful as a way of investigating trends in the unsteady lift, rather than relying on it to give the actual values of unsteady lift.

Some ways of using the predictor include seeing how changes in the axial spacing, blade skew, and stagger angles affect the unsteady lift. The axial spacing in particular can be used to find out how far the rows must be separated in order for the blade interference to become unimportant relative to wake effects. Looking at the plots of the unsteady lift magnitude and phase against radius can show if changes in the skew or stagger angles of the blades will reduce the total unsteady lift. These investigations can give insight into the sources and control of unsteady lift.

As mentioned previously, the use of Mathcad to implement the predictor makes it possible for users to see the algorithms being used and to make minor modifications easily. The basic model could be modified in a number of ways to account for other unsteady lift effects. For instance, the Sears unsteady lift function could be replaced with a different function which accounts for camber and thickness effects. Another possibility is to incorporate empirical lift constants into the calculations in order to make the unsteady lift predictions more accurate.

Finally, the model could be expanded in the future to compute the total unsteady moments acting on the stator and rotor. Currently, the unsteady moment is computed at each radial section, but only the unsteady lift is needed to calculate the total unsteady forces. Computing the total unsteady shaft moment becomes involved because all of the unsteady forces and moments at every section are used. Also, every blade of the row must be accounted for, so an additional phase shift due to the mismatch between the disturbance frequency and the blade rate frequency is needed.

CONCLUSION

A computer model has been developed to compute the unsteady forces acting on a three-dimensional stator-rotor stage using the two-dimensional cascade theory developed by Kemp & Sears (1953,1955). Using Mathcad, graphical output features have been included to show how the unsteady lift varies over the span of a blade. The model can be used as an interactive design tool by turbomachinery designers to estimate the unsteady forces for different blade designs and stage configurations. Since the theory and algorithms are visible to the user, the model can also be used to investigate the unsteady lift calculations and can be used to diagnose unsteady lift problems in a design. Use of the unsteady force predictions can help engineers generate ideas for creating new turbomachinery designs which have lower values of unsteady forces.

REFERENCES

Kemp, N.H. and W.R. Sears, "Aerodynamic Interference Between Moving Blade Rows," *Journal of the Aeronautical Sciences*, Vol. 20, No. 9, pp. 585-597, 1953.

Kemp, N.H. and W.R. Sears, "The Unsteady Forces Due to Viscous Wakes in Turbomachines," *Journal of the Aeronautical Sciences*, Vol. 22, No. 7, pp. 478-484, 1955.

Sears, W.R., "Some Aspects of Non-Stationary Airfoil Theory and its Practical Application," *Journal of the Aeronautical Sciences*, Vol. 8, No. 3, pp. 104-108, 1941.

Sevik, M., "Blade Interactions in Axial Flow Machines," ORL Unclassified TM 549.3411-02, 3 October 1966.

Parameter	Description
Number of Harmonics	Number of blade rate harmonics calculated
Axial Spacing	Distance between stator stack-up line and rotor stack-up line (include length unit)
RPM	Rotor rotation, revolutions per minute (include units)
Reference Velocity	Free stream fluid velocity (include units)
Fluid Density	Density of the operating fluid (include units)

Table 1. **Control Parameters**, which are entered by hand at the beginning of the document.

| Parameter	Description
# Blades	Number of stator/rotor blades
Tip Radius	Radius measured from centerline to blade tip along the stack-up line (include units)
Hub Radius	Radius measured from centerline to hub along the stack-up line (include units)
Drag Coefficient	Dimensionless input for stator only (used to compute the viscous wake)

Table 2. **Hand-Entered Blade Parameters**, entered at the beginning of the document.

Field	Section Parameter	Normalizing Factor	Description
1	Section Number	(An Index)	Counting index starting at one
2	Radius	Tip Radius	Measured along the radial stack-up line
3	Pitch Distance	Tip Diameter	Axial distance, or advance ratio, due to the twist (stagger angle) about the radial stack-up line
4	Chord Length	Tip Diameter	Distance between the leading and trailing edges of the section
5	Skew Angle	(Degrees)	Tangential angular displacement of the section, positive when opposite the direction of the rotor rotation
6	*Maximum Camber*	Tip Diameter	Not used by Kemp-Sears Predictor
7	*Maximum Thickness*	Tip Diameter	Not used by Kemp-Sears Predictor
8	Rake	Tip Diameter	Axial displacement of the section, positive when in the direction of the flow (downstream)
9	*Lift Curve Slope*		Not used by Kemp-Sears Predictor

Table 3. **Blade Section Data Input File Format.** The data file must be in ASCII format and contain one section per line (so there will be nine fields per line). The fields can be separated by spaces, tabs, or commas, since Mathcad will consider any of these as valid field delimiters.

Variable	Name	Relationship to Three-Dimensional Blade
Stagger Angle	αs, αr	Calculated from the blade section pitch
Semi-Chord Length	Cs, Cr	One-half the section chord
Separation of Blades (Cascade Pitch)	Ds, Dr	Calculated by dividing the section circumference by the number of blades
Skew	ψs, ψr	Skew of the radial section
Distance Between Rows	B	Axial spacing at the hub, plus the rotor section rake minus the stator section rake

Table 4. **Cascade Representation Variables,** showing their Mathcad name and their relationship to a radial section of a three-dimensional blade.
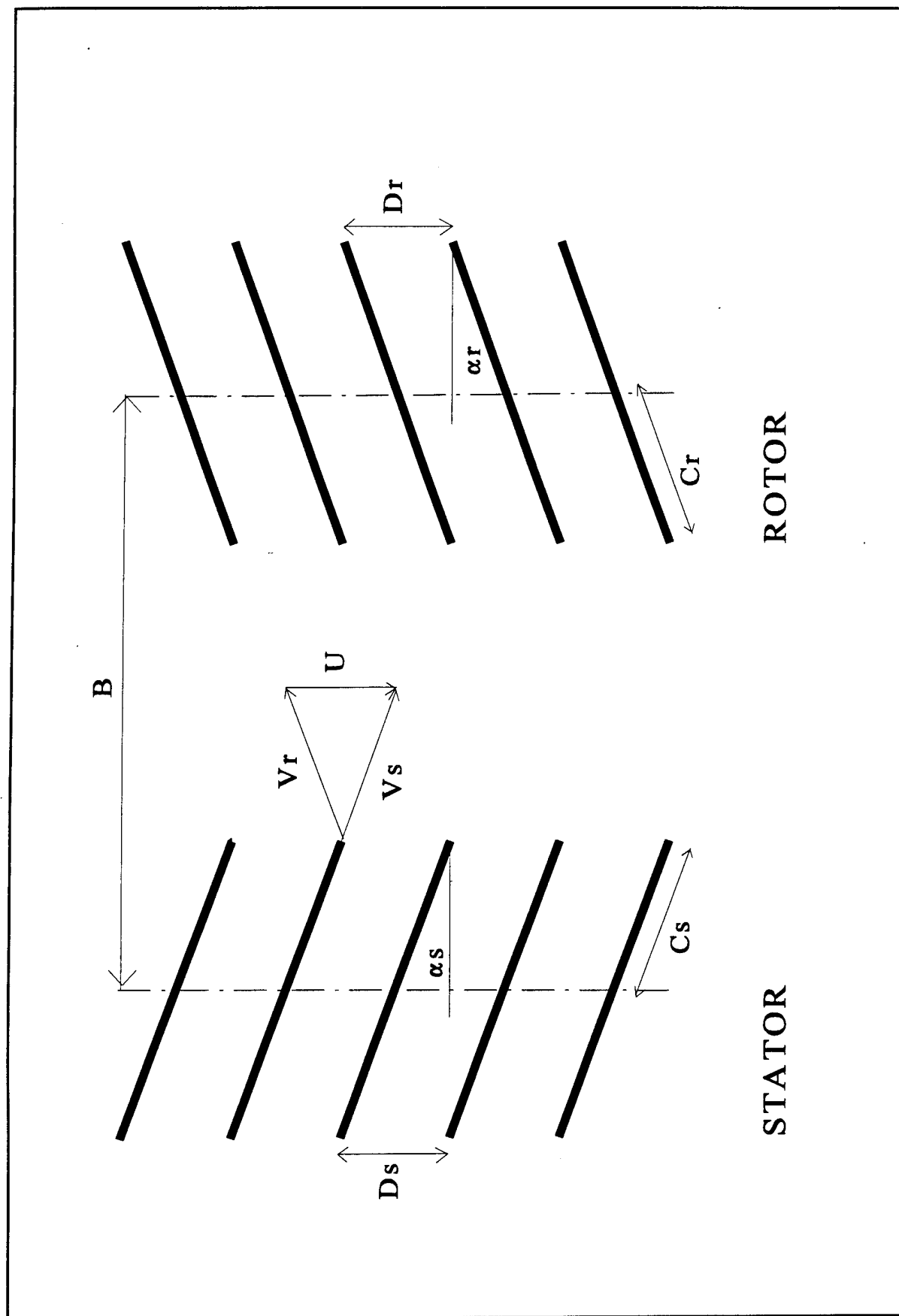
Figure 1. **Cascade Representation of a Radial Section.** The velocity triangle is controlled by the geometry of the cascade, since the flow is assumed to be parallel to the stator and rotor blades.
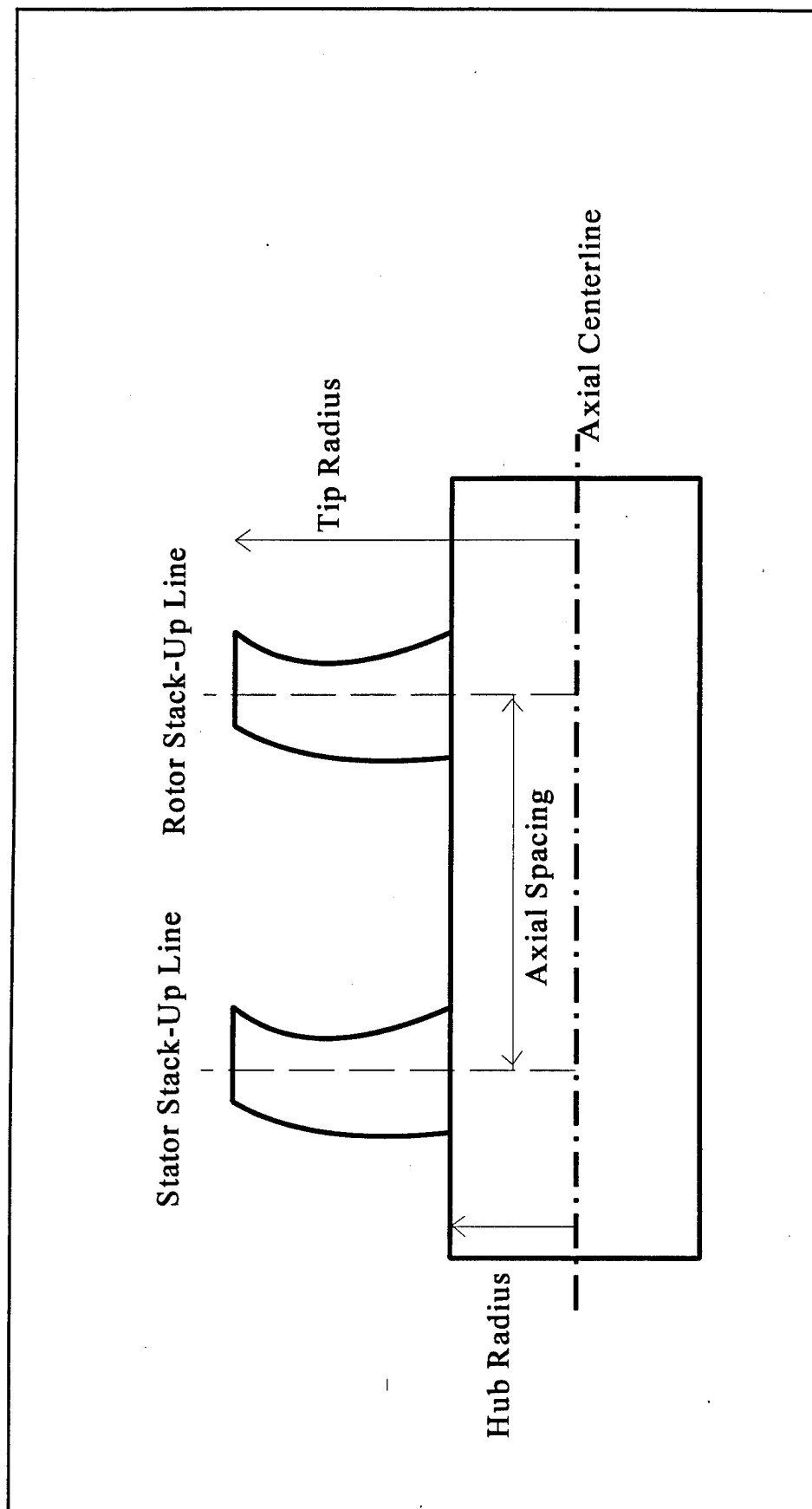
Figure 2.   **Stator-Rotor Setup.**
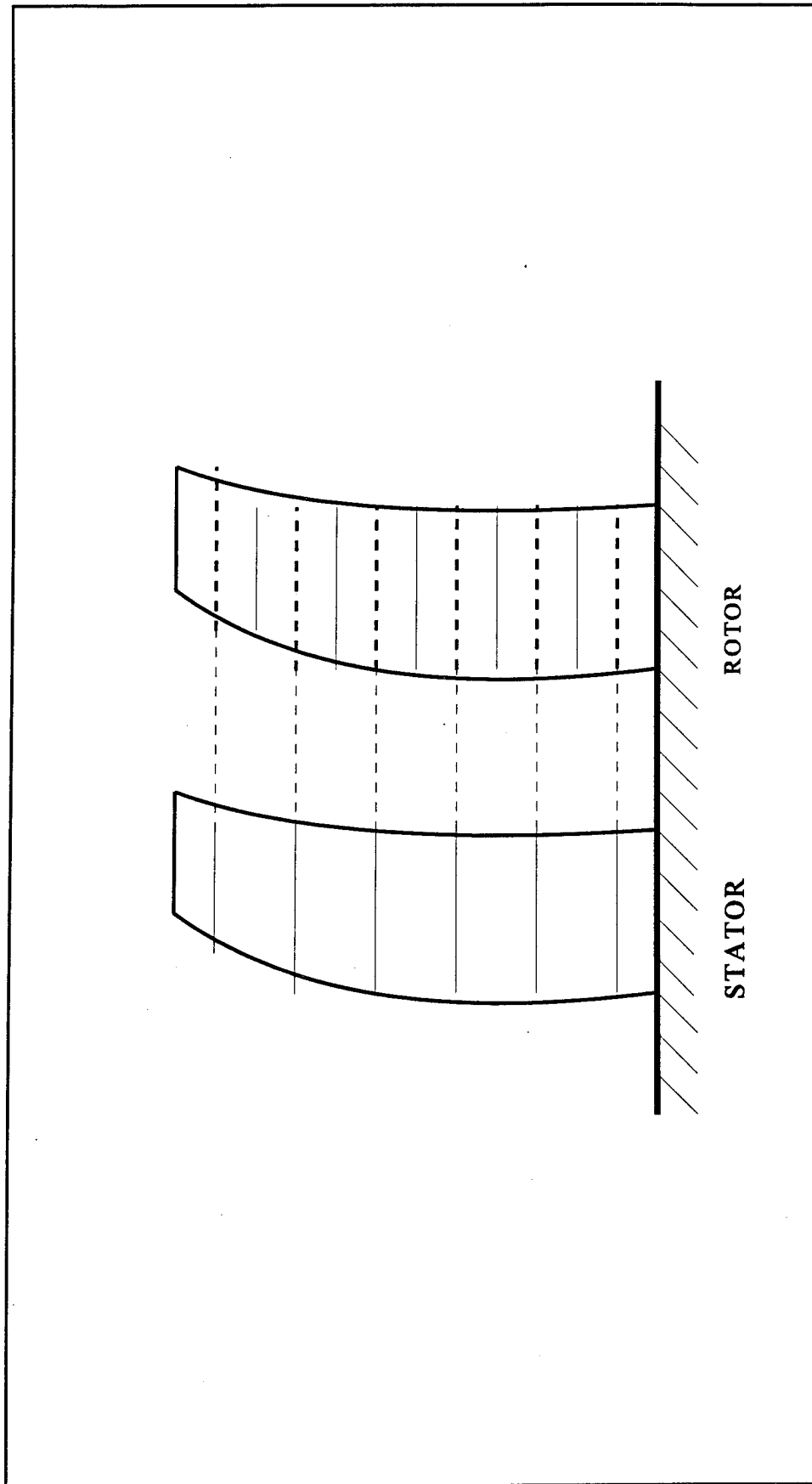
Figure 3. **Geometry Interpolation.** The solid lines are the sections defined in the input files. The dashed lines on the rotor are the sections which are spline interpolated, so both the stator and rotor sections have the same radii. These sections are used to form the cascade representations.

Blade Design ABC								
#	Rad	Pitch	Chord	Skew	Cam	Th	Rake	LC
1	0.18	1.20	0.125	0	0	0	0.00	0
2	0.31	1.18	0.130	5	0	0	0.10	0
3	0.43	1.17	0.132	10	0	0	0.11	0
4	0.55	1.16	0.135	15	0	0	0.12	0
5	0.72	1.17	0.132	20	0	0	0.13	0
6	0.90	1.15	0.125	25	0	0	0.14	0
7	1.00	1.13	0.115	30	0	0	0.15	0

A valid blade input file.

```
Blade Design ABC
1, 0.18, 1.20, 0.125, 0, 0.12, 0.05, 0.00, 6.28
2, 0.35, 1.18, 0.130, -5, 0.11, 0.06, 0.10, 6.28
3, 0.67, 1.17, 0.132, -10, 0.10, 0.06, 0.11, 6.28
4, 0.95, 1.16, 0.135, -15, 0.09, 0.05, 0.12, 6.28
```

Another valid blade input file.

Blade Design 1234								
1	0.18	1.20	0.125	0	0	0	0.00	0
2	0.31	1.18	0.130	5	0	0	0.10	0
3	0.53	1.17	0.132	10	0	0	0.11	0
4	0.95	1.16	0.135	15	0	0	0.12	0

An invalid blade input file, since there cannot be any number fields before the data.

Figure 4.   **Sample Blade Input Files.**

APPENDIX A.

KEMP-SEARS PREDICTOR NOMENCLATURE

NOTES:

The letters r and s are used as prefixes and suffixes to denote rotor and stator blades, respectively. Small r and s are used for cascade variables and other variables used in the Kemp-Sears calculation section to avoid confusion with the subscript capital R (used for radial section). Capital S and R are used for other blade geometry variables not involved in the Kemp-Sears calculation section.

Three subscripts are used as indexes for arrays. R is used for radial section, m is used for harmonic, and k is used for the potential wake series.

NAME	DESCRIPTION
αr	rotor stagger angle at interpolated sections
αs	stator section stagger angle
β	sum of stator and rotor section stagger angles
Γ	ratio of rotor to stator steady circulation
Γr	ratio of rotor time-dependent to steady circulation
Γs	ratio of stator time-dependent to steady circulation
λr	rotor section complex frequency
λs	stator section complex frequency
ρ	fluid density
σr	rotor section solidity (2Cr/Dr)
σs	stator section solidity (2Cs/Ds)
$\phi(\text{fnct})$	the phase angle of a complex number
ϕpR	rotor pitch angle at interpolated sections
ϕpS	stator section pitch angle
ψr	rotor skew angle at interpolated sections
ψs	stator section skew angle
ωr	rotor section reduced frequency
ωs	stator section reduced frequency
A0r	rotor steady bound vortex coefficient (default=0)
A0s	stator steady bound vortex coefficient (default=0)

NAME	DESCRIPTION
A1r	rotor steady bound vortex coefficient (default=1, elliptical distribution)
A1s	stator steady bound vortex coefficient (default=1, elliptical distribution)
Ang_Vel	rotor angular velocity
Ar	area of rotor blade
As	area of stator blade
B	section axial distance between blade rows
B_axial	axial spacing, stator stack-up line to rotor stack-up line
BladesR	number of rotor blades
BladesS	number of stator blades
$C(\omega)$	Theodorsen function
CDS	stator drag coefficient
cJ(z)	cJ0(z) - i cJ1(z)
cJ0(z)	Bessel function J0 for complex z
cJ1(z)	Bessel function J1 for complex z
Cr	rotor section semi-chord length at interpolated sections
Cs	stator section semi-chord length
Dr	rotor section cascade pitch (distance between adjacent blades)
Ds	stator section cascade pitch
expon	argument used in Grv
Fr	rotor coefficient of quasi-steady circulation
Fs	stator coefficient of quasi-steady circulation
Gr	rotor coefficient of velocity induced at blade
Gr2	rotor coefficient of velocity induced at blade due to potential wake
Grv	rotor coefficient of velocity induced at blade due to viscous wake
Gs	stator coefficient of velocity induced at blade
h	harmonic for which the plots are displayed
Hr	rotor steady bound vortex distribution function

NAME	DESCRIPTION
Hr2	Hr used in potential wake calculation
Hs	stator steady bound vortex distribution function
ii	index, 2 to R_tot - 1
J(z)	J0(z) - i J1(z)
k	index for potential wake series (1 to K_tot)
K_tot	number of terms used in potential wake series
K0(z)	modified Bessel function
K1(z)	modified Bessel function
$K_L(\omega,\lambda)$	lift function
$K_M(\omega,\lambda)$	moment function
m	index for harmonics
M_tot	number of harmonics calculated
pitchR	rotor section pitch at interpolated sections
pitchS	stator section pitch
Ps	function used in potential wake calculations
Qm	function used in potential wake calculations
Qp	function used in potential wake calculations
R	index for radial sections (stator and interpolated rotor)
r_ϕL	rotor unsteady lift phase for harmonic h
r_ϕLift(r)	smooth function of r_ϕL for plots
R_ψ_int(r)	function used to find an interpolated rotor skew
R_ψ_orig	array of rotor section skew angles stored in blade file
R_c_int(r)	function used to find an interpolated rotor chord length
R_c_orig	array of rotor section chord lengths stored in blade file
R_i	array of section numbers for rotor
r_L	unsteady rotor lift magnitude per span for harmonic h
R_lift	rotor unsteady lift at each section (not coefficient)

NAME	DESCRIPTION
r_Lift(r)	smooth function of r_L for plots
R_Lx	total rotor blade unsteady force coefficient acting in tangential direction
R_Lz	total rotor blade unsteady force coefficient acting in axial direction
R_pitch_int(r)	function to find interpolated pitch values
R_pitch_orig	array of rotor section pitch values stored in blade file
R_rad_orig	array of rotor section radii stored in blade file
R_rake_int(r)	function used to find interpolated rake values
R_rake_orig	array of rotor section rake values stored in blade file
R_side_force	total rotor blade unsteady force acting in tangential direction
R_thrust	total rotor blade unsteady force acting in axial direction
rϕ_spline	cubic spline data for r_ϕLift(r)
R2j_arg	argument used in H-function for potential wake
RadR	radii of interpolated rotor sections
RadR_n	radii of rotor sections normalized by tip radius
RadS	radii of stator sections
RadS_n	radii of stator sections normalized by tip radius
rakeR	rotor section rake at interpolated sections
rakeS	stator section rake
Rargm	argument for rotor coefficient of induced velocity (Gr)
RhR	rotor hub radius
RhS	stator hub radius
Rj_arg	argument for rotor bound-vortex distribution function (Hr)
rL_spline	cubic spline data for r_Lift(r)
RL1	rotor section unsteady lift coefficient due to non-steady flow
RL2	rotor section unsteady lift coefficient due to potential wake
RLt	rotor section unsteady lift coefficient due to all three effects
RLv	rotor section unsteady lift coefficient due to viscous wake

NAME	DESCRIPTION
RM1	rotor section unsteady moment coefficient due to non-steady flow
RM2	rotor section unsteady moment coefficient due to potential wake
RMt	rotor section unsteady moment coefficient due to all three effects
RMv	rotor section unsteady moment coefficient due to viscous wake
Rotor_Geom	matrix holding all the denormalized data from the geometry file
RPM	revolutions per minute (rotor)
RpR	tip radius of the rotor
RpS	tip radius of the stator
r_r (range)	range of normalized rotor radii to make smooth plots
r_s (range)	range of normalized stator radii to make smooth plots
$S(\omega)$	Sears function
s_ϕL	stator unsteady lift phase for harmonic h
s_ϕLift(r)	smooth function of s_ϕL for plots
S_ψ_orig	array of stator section skew angles
S_c_orig	array of stator chord lengths
S_i	array of section numbers for stator
S_L	unsteady stator lift magnitude per span for harmonic h
S_lift	stator unsteady lift at each section (not coefficient)
s_Lift(r)	smooth function of s_L for plots
S_Lx	total stator blade unsteady force coefficient acting in tangential direction
S_Lz	total stator blade unsteady force coefficient acting in axial direction
S_pitch_orig	array of stator section pitch values
S_rad_orig	array of radii corresponding to each section of the stator blade
S_rake_orig	array of stator section rake values
S_side_force	total stator blade unsteady force acting in tangential direction
S_thrust	total stator blade unsteady force acting in axial direction
sϕ_spline	cubic spline data for s_ϕLift(r)

NAME	DESCRIPTION
Sargm	argument for stator coefficient of induced velocity (Gs)
Sj_arg	argument for stator steady bound vortex function (Hs)
SL	stator section unsteady lift coefficient
sL_spline	cubic spline data for S_Lift(r)
SM	stator section unsteady moment coefficient
Span	radial length of each sectional strip
Stator_Geom	matrix holding all denormalized geometry data from the file
U	wheel speed of rotor, linear cascade equivalent of angular velocity
Vr	speed of flow relative to rotor
Vref	reference (free-stream) velocity
Vs	speed of flow relative to stator
Xo	rotor x-coordinate for viscous wake (default quarter chord)
Xo'	rotor x-coordinate corresponding to Xo in oblique coordinate system

APPENDIX B.

KEMP-SEARS PREDICTOR MATHCAD DOCUMENT

KEMP-SEARS UNSTEADY LIFT AND MOMENT PREDICTOR

HIREP Geometry

UFAM Geometry File Version

# Harmonics:	$M\_tot \equiv 3$

Axial Spacing $B\_axial \equiv 15.88 \cdot in$

This page contains all of the user input variables. The results are on the next page, followed by the calculations.

RPM $RPM \equiv 260 \cdot \dfrac{1}{min}$

Fluid Density $\rho \equiv 1.937 \cdot \dfrac{slug}{ft^3}$ (water)

Reference Velocity $V_{ref} \equiv 35 \cdot \dfrac{ft}{sec}$

Stator Blade Description:

Number of Blades: $BladesS \equiv 13$

Tip Radius: $RpS \equiv 1.75 \cdot ft$

Hub Radius: $RhS \equiv 0.875 \cdot ft$

Stator Drag Coefficient $CDs \equiv 0.002$

Rotor Blade Description:

Number of Blades: $BladesR \equiv 7$

Tip Radius: $RpR \equiv 1.75 \cdot ft$

Hub Radius: $RhR \equiv 0.875 \cdot ft$

Read-in Geometry data from files. Select filenames using *Associate Filename* (File Menu).

$Stator\_Geom \equiv READPRN(stator\_geom)$

$Rotor\_Geom \equiv READPRN(rotor\_geom)$

Section Numbers $S\_i \equiv Stator\_Geom^{<0>}$

$R\_i \equiv Rotor\_Geom^{<0>}$

Section Radius $S\_rad\_orig \equiv Stator\_Geom^{<1>} \cdot RpS$

$R\_rad\_orig \equiv Rotor\_Geom^{<1>} \cdot RpR$

Pitch Distance $S\_pitch\_orig \equiv Stator\_Geom^{<2>} \cdot 2 \cdot RpS$

$R\_pitch\_orig \equiv Rotor\_Geom^{<2>} \cdot 2 \cdot RpR$

Chord Length $S\_c\_orig \equiv Stator\_Geom^{<3>} \cdot 2 \cdot RpS$
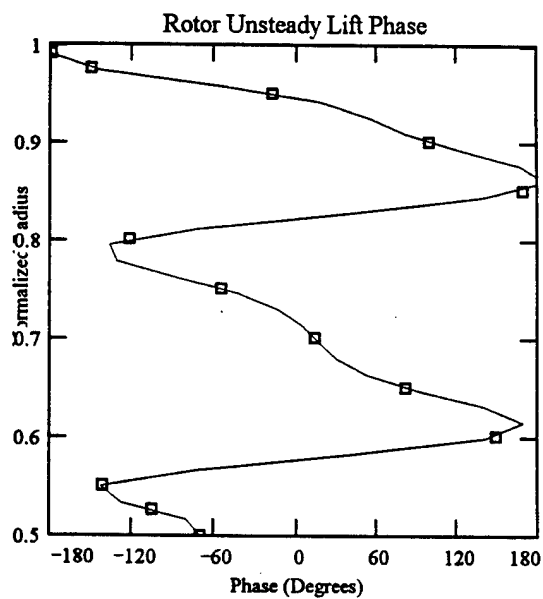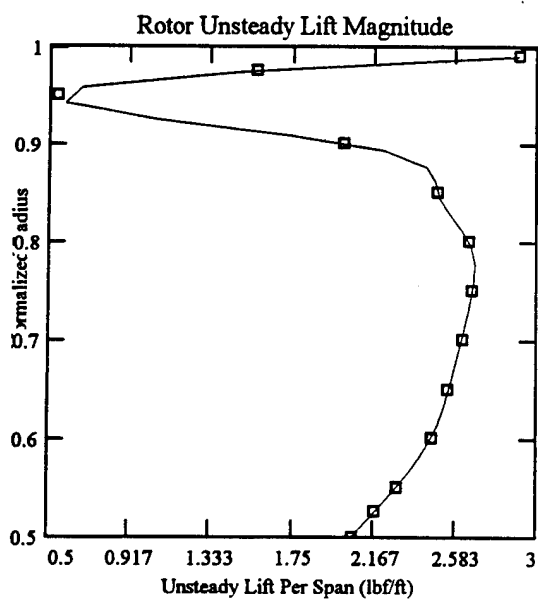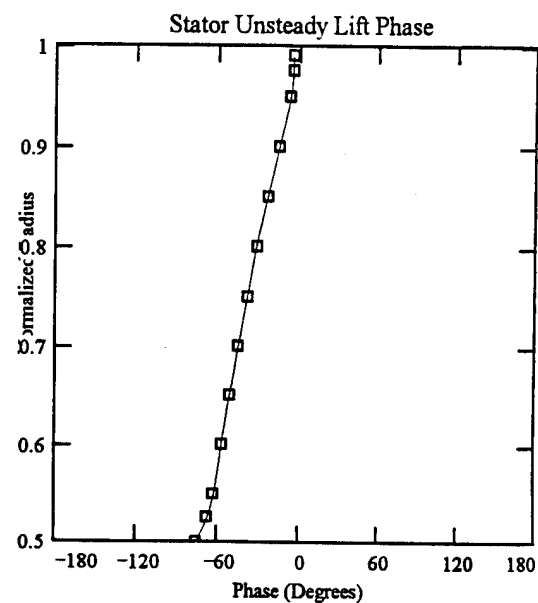
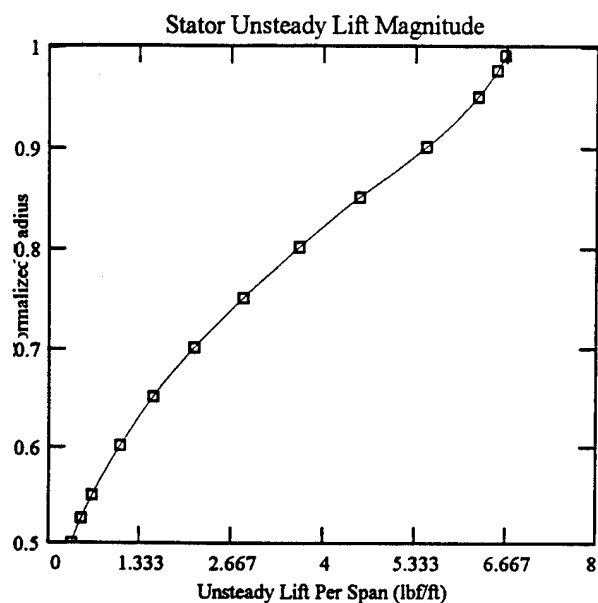$R\_c\_orig \equiv Rotor\_Geom^{<3>} \cdot 2 \cdot RpR$

Skew Angle $S\_\psi\_orig \equiv Stator\_Geom^{<4>} \cdot \dfrac{\pi}{180}$

$R\_\psi\_orig \equiv Rotor\_Geom^{<4>} \cdot \dfrac{\pi}{180}$

Rake $S\_rake\_orig \equiv Stator\_Geom^{<7>} \cdot 2 \cdot RpS$

$R\_rake\_orig \equiv Rotor\_Geom^{<7>} \cdot 2 \cdot RpR$

Unsteady Lift Results

Stator Unsteady Lift Magnitude

Stator Unsteady Lift Phase

Rotor Unsteady Lift Magnitude

Rotor Unsteady Lift Phase

Tables of Total Unsteady Force Coefficients

The total unsteady force coefficients acting on one blade are shown.

Axial Lift Coefficients

Stator

Magnitude $\left\|S\_Lz_m\right\|$	Phase (Degrees) $\phi\left(S\_Lz_m\right)$
$4.18 \cdot 10^{-4}$	150.365
$3.274 \cdot 10^{-6}$	157.978
$4.458 \cdot 10^{-8}$	172.119

Rotor

Magnitude $\left\|R\_Lz_m\right\|$	Phase (Degrees) $\phi\left(R\_Lz_m\right)$
$2.955 \cdot 10^{-4}$	6.519
$9.028 \cdot 10^{-5}$	278.081
$4.902 \cdot 10^{-5}$	249.723

Tangential Lift Coefficients

Stator

Magnitude $\left\|S\_Lx_m\right\|$	Phase (Degrees) $\phi\left(S\_Lx_m\right)$
0.004	156.154
$3.933 \cdot 10^{-5}$	166.906
$5.992 \cdot 10^{-7}$	184.245

Rotor

Magnitude $\left\|R\_Lx_m\right\|$	Phase (Degrees) $\phi\left(R\_Lx_m\right)$
$2.866 \cdot 10^{-4}$	10.319
$6.766 \cdot 10^{-5}$	257.453
$4.437 \cdot 10^{-5}$	283.811

Plots of Total Unsteady Force Results

Stator Unsteady Force Coefficients

Rotor Unsteady Force Coefficients
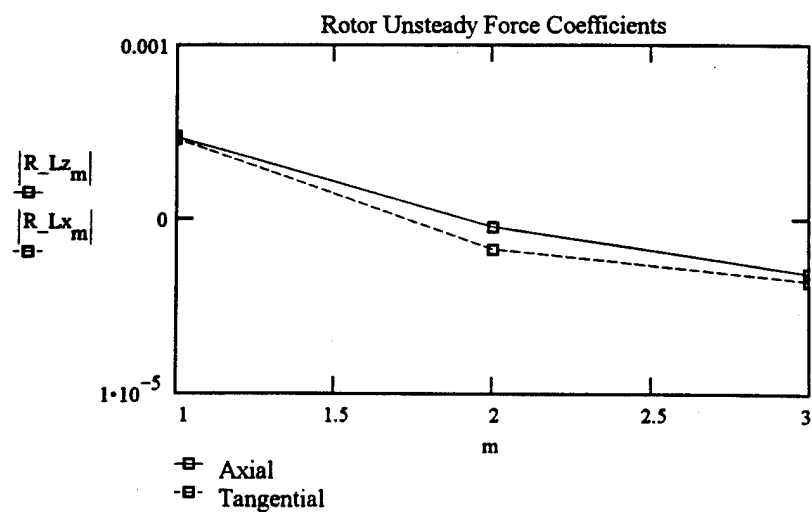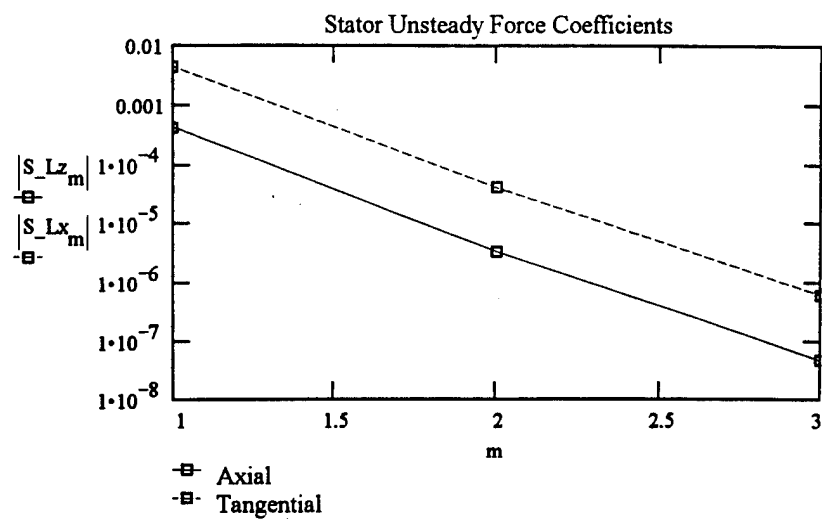
The remainder of the document contains definitions and calculations.

Define coefficients of steady bound-vortex distribution. See p. 594 of Kemp & Sears, 1953.

Use elliptical distribution (A0 = 0) for symmetrical camber with no angle of incidence.

$A0s \equiv 0$ $A0r \equiv 0$

$A1s \equiv 1$ $A1r \equiv 1$

Interpolate rotor geometry to new sections and define stagger angle.

Rotor radial sections moved to the sections defined for the stator $RadR \equiv S\_rad\_orig$

$R\_pitch\_int(r) \equiv interp(cspline(R\_rad\_orig, R\_pitch\_orig), R\_rad\_orig, R\_pitch\_orig, r)$

$\overrightarrow{pitchR \equiv R\_pitch\_int(RadR)}$

$R\_c\_int(r) \equiv interp(cspline(R\_rad\_orig, R\_c\_orig), R\_rad\_orig, R\_c\_orig, r)$

Chord converted to semi-chord

$R\_\psi\_int(r) \equiv interp(cspline(R\_rad\_orig, R\_\psi\_orig), R\_rad\_orig, R\_\psi\_orig, r)$

$Cr \equiv \dfrac{\overrightarrow{R\_c\_int(RadR)}}{2}$

$R\_rake\_int(r) \equiv interp(cspline(R\_rad\_orig, R\_rake\_orig), R\_rad\_orig, R\_rake\_orig, r)$

$\overrightarrow{\psi r \equiv R\_\psi\_int(RadR)}$

$\overrightarrow{rakeR \equiv R\_rake\_int(RadR)}$

Pitch Angle $\overrightarrow{\phi pR \equiv angle(2 \cdot \pi \cdot RadR, pitchR)}$

Stagger Angle $\alpha r \equiv \dfrac{\pi}{2} - \phi pR$

Rename and define variables for stator blade

$RadS \equiv S\_rad\_orig$

$pitchS \equiv S\_pitch\_orig$

$Cs \equiv \dfrac{S\_c\_orig}{2}$

Pitch Angle $\overrightarrow{\phi pS \equiv angle(2 \cdot \pi \cdot RadS, pitchS)}$

$\psi s \equiv S\_\psi\_orig$

Stagger Angle $\alpha s \equiv \dfrac{\pi}{2} - \phi pS$
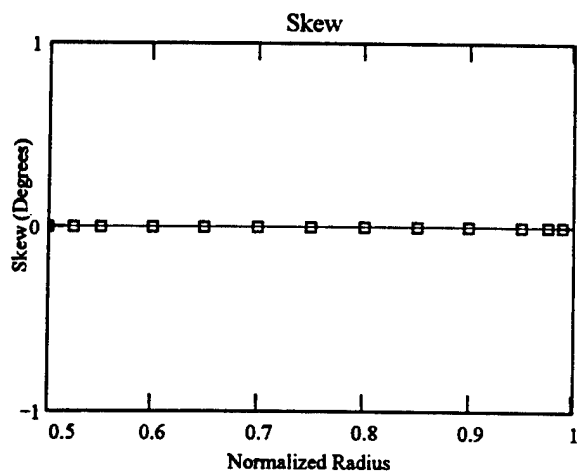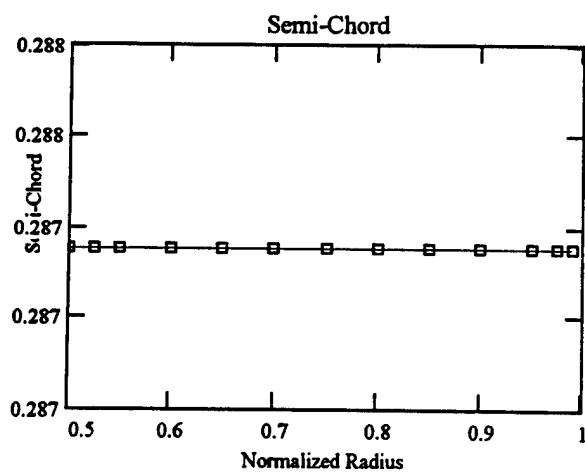
$rakeS \equiv S\_rake\_orig$

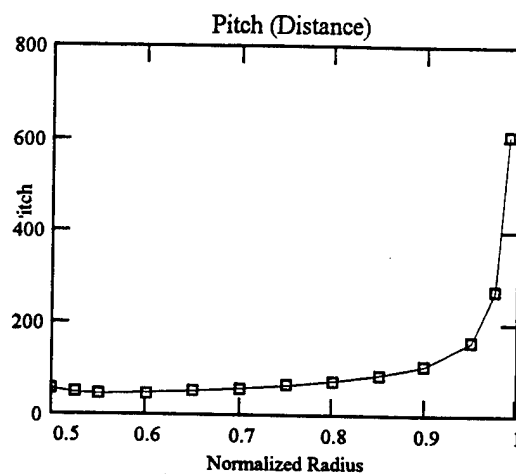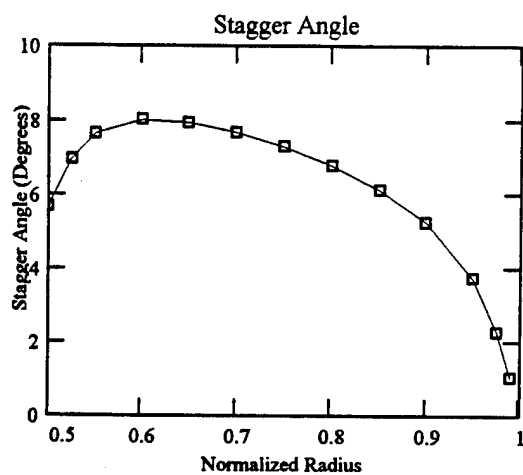## Axial distance between blade rows. (Accounts for the rake of the blades - rake is positive in the direction of the flow).

$\overrightarrow{B \equiv (B\_axial + rakeR - rakeS)}$

Use the next two pages to check the blade geometries.

STATOR

Stagger Angle

Pitch (Distance)

Semi-Chord

Skew

Rake
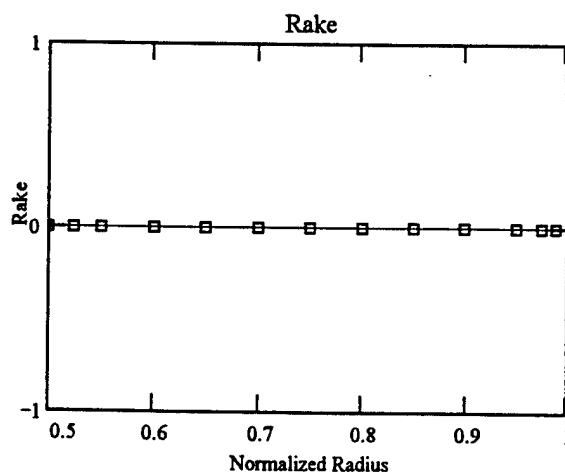
Check interpolated rotor points compared to the original points defined in the geometry file.

ROTOR

Box   Interpolated Point
+   Point from Geometry File
Line   Cubic Spline Interpolated Curve

Stagger Angle

Pitch (Distance)

Semi-Chord

Skew

Rake
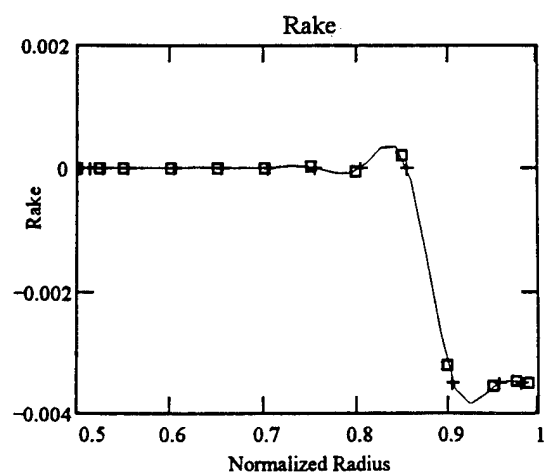
Variable definitions:

ORIGIN ≡ 1

Number of Radial Sections: $R\_tot \equiv rows(RadS)$ $R \equiv 1 .. R\_tot$ The number of radial sections is found automatically from the input variables.

Harmonic range: $m \equiv 1 .. M\_tot$

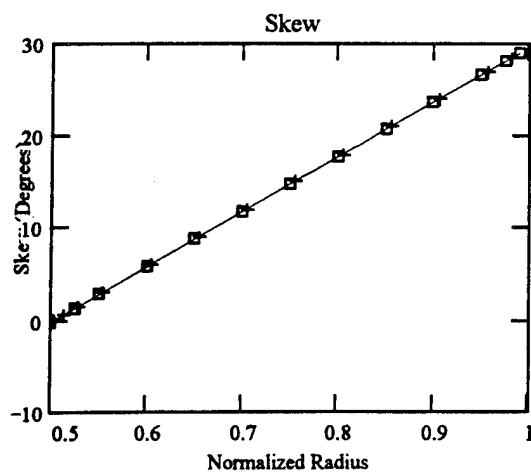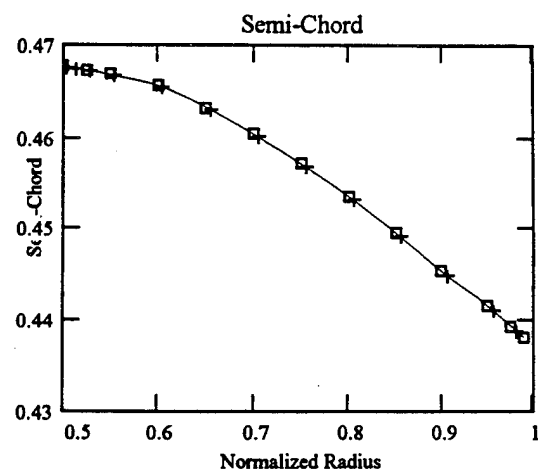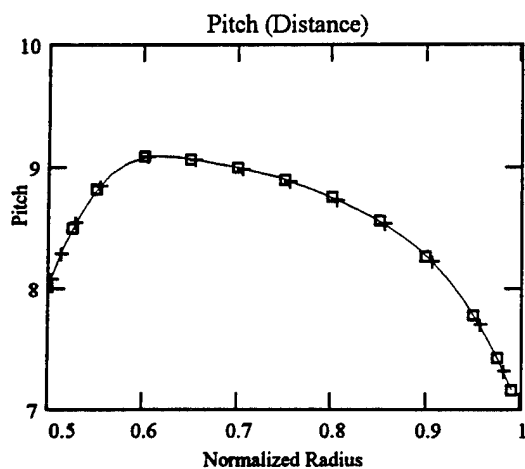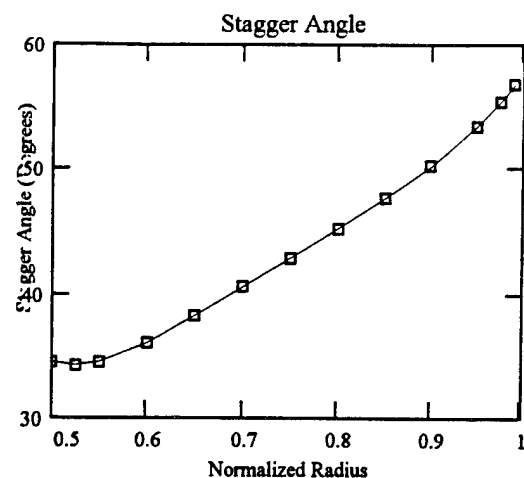**# Terms in Potential Wake Series:** $K\_tot \equiv 3$ $k \equiv 1 .. K\_tot$ Three potential wake terms are probably sufficient, but more terms could be calculated if desired by changing K_tot.

Sum of Angles: $\beta \equiv \alpha s + \alpha r$

Distance between blades in a given row (called pitch by Kemp & Sears): $Ds \equiv \dfrac{2 \cdot \pi \cdot RadS}{BladesS}$ $Dr \equiv \dfrac{2 \cdot \pi \cdot RadR}{BladesR}$

Rotor x-coordinate, measured along the airfoil from mid-chord, used in viscous wake calculation: $Xo \equiv \dfrac{Cr}{2}$ The X coordinate is assumed to be at the quarter chord length. See page 480 and 482 of Kemp & Sears, 1955.

Ratio of steady circulations, rotor over stator: $\Gamma \equiv \overrightarrow{\left(-\dfrac{Dr}{Ds}\right)}$ See equation 60, page 594 of Kemp & Sears, 1953.

More Variable definitions:

Angular velocity of rotor:

$$Ang\_Vel \equiv RPM \cdot 2 \cdot \pi$$

Wheel Speed:

$$U \equiv RadR \cdot Ang\_Vel$$

Speed of flow (relative to stator):

$$\overrightarrow{Vs \equiv \left(U \cdot \frac{\cos(\alpha r)}{\sin(\alpha r) \cdot \cos(\alpha s) + \cos(\alpha r) \cdot \sin(\alpha s)} \right)}$$

Speed of flow (relative to rotor):

$$\overrightarrow{Vr \equiv \left(U \cdot \frac{\cos(\alpha s)}{\sin(\alpha r) \cdot \cos(\alpha s) + \cos(\alpha r) \cdot \sin(\alpha s)} \right)}$$

Solidities:

$$\overrightarrow{\sigma s \equiv \left(2.0 \cdot \frac{Cs}{Ds} \right)} \qquad\qquad \overrightarrow{\sigma r \equiv \left(2.0 \cdot \frac{Cr}{Dr} \right)}$$

Reduced Frequencies:

$$\overrightarrow{\omega s \equiv \left(2 \cdot \pi \cdot \frac{U}{Dr} \cdot \frac{Cs}{Vs} \right)} \qquad\qquad \overrightarrow{\omega r \equiv \left(2 \cdot \pi \cdot \frac{U}{Ds} \cdot \frac{Cr}{Vr} \right)}$$

From equations 44, 49:

$$\overrightarrow{\lambda s \equiv \left[\frac{2 \cdot \pi \cdot Cs}{Dr} \cdot e^{i \cdot \left(\frac{\pi}{2} - \alpha s \right)} \right]} \qquad\qquad \overrightarrow{\lambda r \equiv \left[\frac{2 \cdot \pi \cdot Cr}{Ds} \cdot e^{-i \cdot \left(\frac{\pi}{2} - \alpha r \right)} \right]}$$

Definition of functions:

Bessel functions with complex arguments:

$$cJ0(z) \equiv \frac{1}{\pi} \cdot \int_0^\pi \cos(z \cdot \sin(\theta)) \, d\theta \qquad\qquad cJ1(z) \equiv \frac{1}{\pi} \cdot \int_0^\pi \cos(z \cdot \sin(\theta) - \theta) \, d\theta$$

$$K0(z) \equiv -\frac{\pi}{2} \cdot i \cdot (J0(z) - i \cdot Y0(z)) \qquad\qquad K1(z) \equiv -\frac{\pi}{2} \cdot (J1(z) - i \cdot Y1(z))$$

Theodorsen function:
$$C(\omega) \equiv \frac{K1(\omega)}{K0(\omega) + K1(\omega)}$$

Sears function:
$$S(\omega) \equiv \frac{1}{i \cdot \omega \cdot (K0(\omega) + K1(\omega))}$$

From equation 10.
$$J(z) \equiv J0(z) - i \cdot J1(z)$$

$$cJ(z) \equiv cJ0(z) - i \cdot cJ1(z)$$

Lift and Moment functions (equations 16 and 17).

$$K_L(\omega, \lambda) \equiv cJ(\lambda) \cdot C(\omega) + i \cdot \frac{\omega}{\lambda} \cdot cJ1(\lambda)$$

$$K_M(\omega, \lambda) \equiv cJ(\lambda) \cdot (C(\omega) - 1) + \frac{\omega}{\lambda} \cdot cJ0(\lambda) + \frac{2}{\lambda} \cdot \left(1 - \frac{\omega}{\lambda}\right) \cdot cJ1(\lambda)$$

Unsteady Stator Lift.

Reference: Kemp, N.H. and W.R. Sears, *Aerodynamic Interference Between Moving Blade Rows*, 1953.

Calculate steady bound-vortex distribution function (Hr) for the rotor, based on equation 31.

$$Rj\_arg_{R,m} \equiv m \cdot \pi \cdot \sigma_{T_R} \cdot e^{-i \cdot \left(\frac{\pi}{2} - \alpha r_R\right)}$$

$$Hr_{R,m} \equiv \frac{A0r}{A0r + A1r} \cdot \left(cJ0\left(Rj\_arg_{R,m}\right) + i \cdot cJ1\left(Rj\_arg_{R,m}\right)\right) + 2 \cdot i \cdot \frac{e^{-i \cdot \alpha r_R}}{\pi \cdot \sigma_{T_R} \cdot m} \cdot \frac{A1r}{A0r + A1r} \cdot cJ1\left(Rj\_arg_{R,m}\right)$$

Calculate coefficient of velocity induced at blade (Gs) for the stator, based on equation 37.

$$Sargm_{R,m} \equiv -\pi \cdot m \cdot \sigma_{T_R} \cdot \left[\frac{B_R}{Cr_R} \cdot \left(1.0 + i \cdot \tan\left(\alpha r_R\right) - i \cdot \frac{U_R}{Vs_R \cdot \cos\left(\alpha s_R\right)}\right) - i \cdot \frac{U_R}{Vr_R}\right]$$

$$Gs_{R,m} \equiv \pi \cdot \sigma s_R \cdot \frac{Ds_R}{Dr_R} \cdot e^{-i \cdot \alpha s_R} \cdot Hr_{R,m} \cdot e^{Sargm_{R,m}}$$

Calculate the unsteady stator lift and moment coefficients, based on equations 45 and 46.

$$SL_{R,m} \equiv \Gamma_R \cdot Gs_{R,m} \cdot K_L\left(\omega s_R \cdot m, \lambda s_R \cdot m\right) \cdot e^{-i \cdot \left(\psi s_R - \psi r_R\right) \cdot m \cdot BladesR}$$

$$SM_{R,m} \equiv \frac{\Gamma_R}{4} \cdot Gs_{R,m} \cdot K_M\left(\omega s_R \cdot m, \lambda s_R \cdot m\right) \cdot e^{-i \cdot \left(\psi s_R - \psi r_R\right) \cdot m \cdot BladesR}$$

Calculate the stator coefficient of quasi-steady circulation, based on equation 48.

$$Fs_{R,m} \equiv Gs_{R,m} \cdot cJ\left(\lambda s_R \cdot m\right)$$

Unsteady Rotor Lift due to Non-Steady Flow.

Reference: Kemp, N.H. and W.R. Sears, *Aerodynamic Interference Between Moving Blade Rows*, 1953.

Calculate steady bound vortex distribution function (Hs) for the stator, based on equation 42.

$$Sj\_arg_{R,m} \equiv m \cdot \pi \cdot \sigma s_R \cdot e^{i \cdot \left(\frac{\pi}{2} - \alpha s_R\right)}$$

$$Hs_{R,m} \equiv \frac{A0s}{A0s + A1s} \cdot \left(cJ0\left(Sj\_arg_{R,m}\right) + i \cdot cJ1\left(Sj\_arg_{R,m}\right)\right) - 2 \cdot i \cdot \frac{e^{i \cdot \alpha s_R}}{\pi \cdot \sigma s_R \cdot m} \cdot \frac{A1s}{A0s + A1s} \cdot cJ1\left(Sj\_arg_{R,m}\right)$$

Calculate coefficient of velocity induced at blade (Gr) for the rotor, based on equation 41.

$$Rargm_{R,m} \equiv -\pi \cdot m \cdot \sigma r_R \cdot \frac{Dr_R}{Ds_R} \cdot \left[\frac{B_R}{Cr_R} \cdot \left(1.0 + i \cdot \tan\left(\alpha r_R\right) - i \cdot \frac{U_R}{Vs_R \cdot \cos\left(\alpha s_R\right)}\right) - i \cdot \frac{U_R}{Vr_R}\right]$$

$$Gr_{R,m} \equiv -\pi \cdot \sigma r_R \cdot \frac{Dr_R}{Ds_R} \cdot e^{i \cdot \alpha r_R} \cdot Hs_{R,m} \cdot e^{Rargm_{R,m}}$$

Calculate the unsteady rotor lift and moment coefficients, based on equations 50 and 51.

$$RL1_{R,m} \equiv \frac{1}{\Gamma_R} \cdot Gr_{R,m} \cdot K_L\left(\omega r_R \cdot m, \lambda r_R \cdot m\right) \cdot e^{-i \cdot \left(\psi r_R - \psi s_R\right) \cdot m \cdot BladesS}$$

$$RM1_{R,m} \equiv \frac{1}{4 \cdot \Gamma_R} \cdot Gr_{R,m} \cdot K_M\left(\omega r_R \cdot m, \lambda r_R \cdot m\right) \cdot e^{-i \cdot \left(\psi r_R - \psi s_R\right) \cdot m \cdot BladesS}$$

Calculate the rotor coefficient of quasi-steady circulation, based on equation 53.

$$Fr_{R,m} \equiv Gr_{R,m} \cdot cJ\left(\lambda r_R \cdot m\right)$$

Unsteady Rotor Lift due to Potential Wake Effects.

Reference: Sevik, M. ORL Internal Memorandum, File No. 549.3411-02, 1966, pg. 19.

Calculate rotor steady bound vortex distribution function (Hr2) for the wake series.

$$R2j\_arg_{R,k} \equiv k \cdot \pi \cdot \sigma r_R \cdot e^{-i \cdot \left(\frac{\pi}{2} - \alpha r_R\right)}$$

$$Hr2_{R,k} \equiv \frac{A0r}{A0r + A1r} \cdot \left(cJ0\left(R2j\_arg_{R,k}\right) + i \cdot cJ1\left(R2j\_arg_{R,k}\right)\right) + 2 \cdot i \cdot \frac{e^{-i \cdot \alpha r_R}}{\pi \cdot \sigma r_R \cdot k} \cdot \frac{A1r}{A0r + A1r} \cdot cJ1\left(R2j\_arg_{R,k}\right)$$

Calculate the P-function for the stator.

$$Ps_{R,k} \equiv \pi \cdot \sigma s_R \cdot \frac{Ds_R}{Dr_R} \cdot e^{-i \cdot \alpha s_R} \cdot Hr2_{R,k} \cdot S\left(\omega s_R \cdot k\right) \cdot cJ\left(\lambda s_R \cdot k\right) \cdot e^{-\pi \cdot \sigma r_R \cdot k \cdot \frac{B_R}{Cr_R} \cdot \left(1 + i \cdot \tan\left(\alpha r_R\right)\right)}$$

Calculate the G-function for the rotor.   NOTE: The summation has been split up into two parts.

$$Qm_{R,m} \equiv \sum_k e^{i \cdot \omega r_R \cdot m} \cdot Ps_{R,k} \cdot \left[\frac{m \cdot Dr_R \cdot Vs_R}{k \cdot Ds_R \cdot Vr_R} \left[1 + \frac{1}{\tan\left(\beta_R\right)^2} \left(1 - \frac{m \cdot Dr_R \cdot Vs_R}{k \cdot Ds_R \cdot Vr_R} \cdot \sec\left(\beta_R\right)\right)^2\right]^{-1}\right]$$

$$QP_{R,m} \equiv \sum_k e^{i \cdot \omega r_R \cdot m} \cdot \overline{Ps_{R,k}} \cdot \left[\frac{m \cdot Dr_R \cdot Vs_R}{k \cdot Ds_R \cdot Vr_R} \left[1 + \frac{1}{\tan\left(\beta_R\right)^2} \left(1 + \frac{m \cdot Dr_R \cdot Vs_R}{k \cdot Ds_R \cdot Vr_R} \cdot \sec\left(\beta_R\right)\right)^2\right]^{-1}\right]$$

$$Gr2_{R,m} \equiv \frac{-\pi \cdot \sigma r_R \cdot Dr_R}{Ds_R \cdot \cos\left(\alpha s_R\right)} \cdot \left(Qm_{R,m} - QP_{R,m}\right)$$

Calculate the unsteady lift and moment coefficients.

$$RL2_{R,m} \equiv Gr2_{R,m} \cdot S\left(\omega r_R \cdot m\right) \cdot e^{-i \cdot \left(\psi r_R - \psi s_R\right) \cdot m \cdot BladesS} \qquad RM2_{R,m} \equiv \frac{1}{4} \cdot RL2_{R,m}$$

Unsteady Rotor Lift due to Viscous Wakes.

Reference: Kemp, N.H. and W.R. Sears, *The Unsteady Forces due to Viscous Wakes in Turbomachines*, 1955.

Calculate the rotor x-coordinate corresponding to Xo in the oblique coordinate system, based on equation 27.

$$Xo'_R \equiv Cr_R \cdot \left(\frac{B_R}{Cr_R \cdot \cos\left(\alpha s_R\right)} + \frac{Xo_R}{Cr_R} \cdot \frac{Vs_R}{Vr_R} \right) - 0.7 \cdot Cs_R$$

Calculate coefficient of velocity induced at blade (Grv), based on equation 29.

$$expon_{R,m} \equiv -\pi \cdot m^2 \cdot \left(\frac{0.68 \cdot \sigma s_R}{\sqrt{2} \cdot \cos\left(\alpha s_R\right)} \right)^2 \cdot CDs \cdot \frac{Xo'_R}{Cs_R}$$

$$Grv_{R,m} \equiv 4 \cdot \pi \cdot \frac{Vs_R}{Vr_R} \cdot \frac{2.42 \cdot \sqrt{CDs} \cdot \sin\left(\beta_R\right)}{\frac{Xo'_R}{Cs_R} + 0.3} \cdot \frac{0.68 \cdot \sigma s_R}{\sqrt{2} \cdot \cos\left(\alpha s_R\right)} \cdot \sqrt{CDs \cdot \frac{Xo'_R}{Cs_R}} \cdot e^{expon_{R,m}}$$

Calculate unsteady lift and moment coefficients, based on equation 33.

$$RLv_{R,m} \equiv Grv_{R,m} \cdot S\left(\omega r_R \cdot m\right) \cdot e^{i \cdot m \cdot \frac{2 \cdot \pi}{Ds_R} \cdot Cr_R \cdot \left(\sin\left(\alpha r_R\right) + \cos\left(\alpha r_R\right) \cdot \tan\left(\alpha s_R\right)\right)} \cdot e^{-i \cdot \left(\psi r_R - \psi s_R\right) \cdot m \cdot BladesS}$$

$$RMv_{R,m} \equiv \frac{1}{4} \cdot RLv_{R,m}$$

The exponential term, although not included in the reference, is included because the viscous wake calculations use a different reference time than the rest of the parts. In the viscous wake part, the stator wake initially intersects the the rotor at mid-chord, while in the other parts it strikes the rotor at the trailing edge. The exponential term shifts the phase of the forces due to the viscous wake.

Calculate Lifts from Lift Coefficients and Total the Forces for the Blad

Calculate the span of each radial strip

$$ii \equiv 2 .. R\_tot - 1$$

$$Span_1 \equiv \frac{RadR_2 - RadR_1}{2} + RadR_1 - RhR$$

$$Span_{ii} \equiv \frac{RadR_{ii+1} - RadR_{ii}}{2} + \frac{RadR_{ii} - RadR_{ii-1}}{2}$$

$$Span_{R\_tot} \equiv RpR - RadR_{R\_tot} + \frac{RadR_{R\_tot} - RadR_{R\_tot-1}}{2}$$

Add up the total rotor lift and moment from the three effects.

$$RLt_{R,m} \equiv RL1_{R,m} + RL2_{R,m} + RLv_{R,m}$$

$$RMt_{R,m} \equiv RM1_{R,m} + RM2_{R,m} + RMv_{R,m}$$

Calculate Unsteady Lift at Each Section

$$S\_lift_{R,m} \equiv SL_{R,m} \cdot \left[\frac{1}{2} \cdot \rho \cdot \left(Vs_R \right)^2 \cdot 2 \cdot Cs_R \cdot Span_R \right]$$

$$R\_lift_{R,m} \equiv RLt_{R,m} \cdot \left[\frac{1}{2} \cdot \rho \cdot \left(Vr_R \right)^2 \cdot 2 \cdot Cr_R \cdot Span_R \right]$$

Interpolate Magnitude and Phase of Stator Unsteady Lift for Plots.

This section produces data for a smooth curve for the stator unsteady lift magnitude and phase plots. A range of points from hub to tip are cubic spline interpolated from the sectional unsteady lift data. The plots, which are shown for one harmonic at a time, are displayed in the *Results* section above.

Harmonic #: $h = 1$

Normalize the radius for the plots.

$$RadS\_n \equiv \frac{RadS}{RpS}$$

Define a range of 30 radii between the minimum and maximum radii given as input.

$$r_s \equiv RadS\_n_1, RadS\_n_1 + \frac{RadS\_n_{R\_tot} - RadS\_n_1}{30} .. RadS\_n_{R\_tot}$$

Interpolate the magnitude of the stator lift for this range of radii, using a spline fit.

$$s\_L_R \equiv \left| \frac{S\_lift_{R,h}}{Span_R} \right|$$

$$sL\_spline \equiv cspline(RadS\_n, s\_L)$$

$$s\_Lift(r_s) \equiv interp(sL\_spline, RadS\_n, s\_L, r_s)$$

Interpolate the phase of the stator lift for this range of radii, using a spline fit.

$$\phi(fnct) \equiv angle(Re(fnct), Im(fnct)) \cdot \frac{180}{\pi}$$

$$s\_\phi L_R \equiv \phi(S\_lift_{R,h})$$

$$s\phi\_spline \equiv cspline(RadS\_n, s\_\phi L)$$

$$s\_\phi Lift(r_s) \equiv interp(s\phi\_spline, RadS\_n, s\_\phi L, r_s)$$

Interpolate Magnitude and Phase of Rotor Unsteady Lift for Plots.

This section interpolates the rotor unsteady lift data for the plots in the *Results* section above.

Harmonic #: $h = 1$

Normalize the radius for the plots.

$$RadR\_n \equiv \frac{RadR}{RpR}$$

Define a range of 30 radii between the minimum and maximum rotor radii given as input.

$$r_r \equiv RadR\_n_1, RadR\_n_1 + \frac{RadR\_n_{R\_tot} - RadR\_n_1}{30} .. RadR\_n_{R\_tot}$$

Interpolate magnitude of rotor lift for this range of radii, using a spline fit.

$$r\_L_R \equiv \left| \frac{R\_lift_{R,h}}{Span_R} \right|$$

$$rL\_spline \equiv cspline(RadR\_n, r\_L)$$

$$r\_Lift(r_r) \equiv interp(rL\_spline, RadR\_n, r\_L, r_r)$$

Interpolate the phase of the rotor lift for this range of radii, using a spline fit.

$$r\_\phi L_R \equiv \phi(R\_lift_{R,h})$$

$$r\phi\_spline \equiv cspline(RadR\_n, r\_\phi L)$$

$$r\_\phi Lift(r_r) \equiv interp(r\phi\_spline, RadR\_n, r\_\phi L, r_r)$$

Calculate Total Unsteady Lift Forces Acting on Each Blade.

In this section, the total blade forces acting in the axial and tangential directions are calculated by summing the sectional unsteady lifts.

STATOR

Axial Direction (Thrust)

$$S\_thrust_m \equiv \sum_R S\_lift_{R,m} \cdot \sin\left(\alpha s_R\right)$$

Tangential Direction (Side Force)

$$S\_side\_force_m \equiv \sum_R S\_lift_{R,m} \cdot \cos\left(\alpha s_R\right)$$

ROTOR

Axial Direction (Thrust)

$$R\_thrust_m \equiv \sum_R R\_lift_{R,m} \cdot \sin\left(\alpha r_R\right)$$

Tangential Direction (Side Force)

$$R\_side\_force_m \equiv \sum_R R\_lift_{R,m} \cdot \cos\left(\alpha r_R\right)$$

Convert Lift Forces to Normalized Coefficient Form

	Stator	**Rotor**

Area of Blade

$$As \equiv \sum_R Span_R \cdot \left(2 \cdot Cs_R\right) \qquad\qquad Ar \equiv \sum_R Span_R \cdot \left(2 \cdot Cr_R\right)$$

$$S\_Lz_m \equiv \frac{S\_thrust_m}{\left(\frac{1}{2} \cdot \rho \cdot V_{ref}^2 \cdot As\right)} \qquad\qquad R\_Lz_m \equiv \frac{R\_thrust_m}{\left(\frac{1}{2} \cdot \rho \cdot V_{ref}^2 \cdot Ar\right)}$$

$$S\_Lx_m \equiv \frac{S\_side\_force_m}{\left(\frac{1}{2} \cdot \rho \cdot V_{ref}^2 \cdot As\right)} \qquad\qquad R\_Lx_m \equiv \frac{R\_side\_force_m}{\left(\frac{1}{2} \cdot \rho \cdot V_{ref}^2 \cdot Ar\right)}$$

Verification of Assumptions.

Reference: Kemp, N.H. and W.R. Sears, *Aerodynamic Interference Between Moving Blade Rows*, 1953.

This section calculates the ratio of the unsteady circulation to the steady circulation. The theory used in determining the stator unsteady forces and the first part of the rotor unsteady forces assumes that the ratios are small. From testing it appears that the unsteady force results are stable until either the rotor or stator has an unsteady to steady circulation ratio of about 0.1 to 0 Results are questionable when the ratio is greater than this range. For more information on this assumption, see page 597 o the reference.

Ratio of time-dependent circulations to steady circulations:

$$\Gamma s_R := \Gamma_R \cdot \sum_m \left(Fs_{R,m} \cdot e^{-i \cdot \omega s_R \cdot m} \cdot S\left(\omega s_R \cdot m\right) \right)$$

$$\Gamma r_R := \frac{1}{\Gamma_R} \cdot \sum_m \left(Fr_{R,m} \cdot e^{-i \cdot \omega r_R \cdot m} \cdot S\left(\omega r_R \cdot m\right) \right)$$

$\left|\Gamma s_R\right|$
$3.435 \cdot 10^{-4}$
$4.666 \cdot 10^{-4}$
$6.083 \cdot 10^{-4}$
$9.402 \cdot 10^{-4}$
0.001
0.002
0.002
0.003
0.004
0.004
0.005
0.005
0.005

$\left|\Gamma r_R\right|$
$4.077 \cdot 10^{-8}$
$7.211 \cdot 10^{-8}$
$1.185 \cdot 10^{-7}$
$2.701 \cdot 10^{-7}$
$5.212 \cdot 10^{-7}$
$9.135 \cdot 10^{-7}$
$1.484 \cdot 10^{-6}$
$2.246 \cdot 10^{-6}$
$3.174 \cdot 10^{-6}$
$4.293 \cdot 10^{-6}$
$5.096 \cdot 10^{-6}$
$5.215 \cdot 10^{-6}$
$5.148 \cdot 10^{-6}$

These values should be less than about 0.1 to verify the assumption.

End of Document.